Complement Deposition on Nanoparticles Can Modulate Immune Responses by Macrophage, B and T Cells

Article *in* Journal of Biomedical Nanotechnology · January 2016

CITATIONS
3

READS
148

11 authors, including:

Kirsten Pondman
St Jansdal Hospital
20 PUBLICATIONS **314** CITATIONS
SEE PROFILE

Anthony Tsolaki
Brunel University London
41 PUBLICATIONS **1,848** CITATIONS
SEE PROFILE

Basudev Paudyal
Brunel University, Kingston university
12 PUBLICATIONS **50** CITATIONS
SEE PROFILE

Mohamed H Shamji
Imperial College London
169 PUBLICATIONS **1,904** CITATIONS
SEE PROFILE

Article

Journal of
Biomedical Nanotechnology
Vol. 12, 197–216, 2016
www.aspbs.com/jbn

Complement Deposition on Nanoparticles Can Modulate Immune Responses by Macrophage, B and T Cells

Kirsten M. Pondman[1,2], Anthony G. Tsolaki[1], Basudev Paudyal[1,3], Mohamed H. Shamji[4,5], Amy Switzer[4,5], Ansar A. Pathan[1], Suhair M. Abozaid[1], Bennie Ten Haken[2], Gudrun Stenbeck[3], Robert B. Sim[6], and Uday Kishore[1,*]

[1] *Centre for Infection, Immunity and Disease Mechanisms, College of Health and Life Sciences, Brunel University London, Uxbridge, UB8 3PH, UK*
[2] *Neuro Imaging, MIRA Institute, University of Twente, 7522 NB, Enschede, The Netherlands*
[3] *Department of Life Sciences, College of Health and Life Sciences, Brunel University London, Uxbridge UB8 3PH, UK*
[4] *Allergy and Clinical Immunology, National Heart and Lung Institute, Imperial College London, London, SW3 6LY, UK*
[5] *MRC and Asthma UK Centre in Allergic Mechanisms of Asthma, London, W2 1NY, UK*
[6] *Department of Pharmacology, Oxford University, Mansfield Road, Oxford, OX1 3QT, UK*

Nanoparticles are attractive drug delivery vehicles for targeted organ-specific as well as systemic therapy. However, their interaction with the immune system offers an intriguing challenge to the success of nanotherapeutics *in vivo*. Recently, we showed that pristine and derivatised carbon nanotubes (CNT) can activate complement mainly via the classical pathway leading to enhanced uptake by phagocytic cells, and transcriptional down-regulation of pro-inflammatory cytokines. Here, we report the interaction of complement-activating CMC-CNT and RNA-CNT, and non-complement-activating gold-nickel (Au–Ni) nanowires with cell lines representing macrophage, B and T cells. Complement deposition considerably enhanced uptake of CNTs by immune cells known to overexpress complement receptors. Real-Time qPCR and multiplex array analyses showed complement-dependent down-regulation of TNF-α and IL-1β and up-regulation of IL-12 by CMC- and RNA-CNTs, in addition to revealing IL-10 as a crucial regulator during nanoparticle-immune cell interaction. It appears that complement system can recognize molecular patterns differentially displayed by nanoparticles and thus, modulate subsequent processing of nanoparticles by antigen capturing and antigen presenting cells, which can shape innate and adaptive immune axes.

KEYWORDS: *Nanoparticles, Carbon Nanotubes, Complement, Cytokines, Phagocytosis, Macrophage, Lymphocytes, B Cells.*

INTRODUCTION

Nanoparticles are attractive drug delivery vehicles with a number of biomedical applications.[1] Although most nanotherapeutics are systemically administrated, the target for therapy is mostly designed to be organ- or tissue-specific.[2–4] In some instances, even intracellular delivery is essential,[5] as in the case of gene therapy.[6–8] Due to their advantageous properties, carbon nanotubes (CNTs) have been extensively explored for a range of biomedical applications,[9–11] including drug delivery,[10–16] and *in vivo* imaging.[17,18] The effectiveness of nanoparticles as intravenous drug delivery platforms is dictated by their rapid elimination via the immune cells, which can otherwise lead to potentially hazardous inflammatory responses. Therefore, understanding the interactions between nanoparticles and the immune system is essential for designing their systemic and organ/tissue specific use for *in vivo* delivery.[19]

The innate immune system plays a key role in the clearance of pathogens and synthetic particles including nanoparticles.[20–23] Activation of the complement system, a major humoral component of the innate immunity,[24]

*Author to whom correspondence should be addressed.
Emails: uday.kishore@brunel.a.uk, ukishore@hotmail.com
Received: 21 July 2014
Revised/Accepted: 21 December 2014

can influence therapeutic effectiveness of nanoparticles, as it coats the surface of the nanoparticles with opsonic fragments (mainly C3b), labeling them for recognition, adherence and clearance by phagocytic cells. Of the three complement pathways, the classical pathway starts by binding of C1q to targets including CNTs[22] (charge pattern) either directly, or via adaptor proteins (antibodies and pentraxins).[25] Binding of C1q causes activation of C1r and C1s, which catalyzes cleavage of C2 and C4, leading to the formation of C4bC2a, a surface bound C3 convertase. The lectin pathway recognizes a different range of target ligands, via the recognition subcomponents Mannose-binding lectin (MBL), the ficolins, or Collectin 11. The MBL binding to a carbohydrate array leads to its association with the MBL-associated serine proteases (MASP-2), which in turn, activates C2 and C4, and forming C4bC2a. The alternative pathway involves spontaneous cleavage of C3, generating C3b, which binds directly onto surfaces, including those of microbes and modified (non-pristine) CNTs.[26–28] Surface-bound C3b binds factor B, which is cleaved by factor D, forming C3bBb complexes, the C3 convertase. This generates more C3b, which can bind to the same surface. Binding of C3b to the convertases, forming C4b2a3b and $C3b_2Bb$, which now cleaves C5 to C5b, forms a complex with C6, C7, C8 and C9, known as the membrane attack complex (MAC).[24] The MAC can form pores in the membrane of cellular targets. The formation of MAC on the surface of CNTs may potentially cause damage to tissue in the direct environment.[29] In addition, the smaller cleaved by-products C3a, C4a and C5a generated during the complement activation are potent anaphylatoxins for infiltrating immune cells contributing to inflammation.[22–24, 30]

Non-functionalized, and thus, highly hydrophobic CNTs activate complement via the classical and (to a lesser extent) the alternative pathway.[22] Functionalization of CNTs in order to increase their dispersability and biocompatibility[10, 31–33] can affect both the extent and the pathway of complement activation.[21, 26, 32] For instance, PEGylation, commonly used to limit protein interactions with the nanoparticles increases biocompatibility, and prolongs the circulation time in blood.[34] However, it can also activate complement via the lectin pathway.[26, 35] CNTs, in general, are widely considered to activate complement.[21, 23, 26, 27, 29, 30, 35–39]

As elongated nanoparticles with an aspect ratio similar to asbestos, CNTs are often considered more hazardous than other types of nanoparticles. Longer CNTs appear to trigger more profound cytotoxic responses.[40–44] Evidence of frustrated phagocytosis by Peripheral blood mononuclear cells (PBMCs) and THP-1 cells have been found when straight and individually dispersed CNTs are used; the effect correlated with generation of superoxide anion and TNF-α release.[45] Palomaki et al.[43] showed that all CNTs induced IL-1β secretion by human macrophages, indicating NOD-like receptor family, pyrin domain containing 3 (NLRP3) inflammasome formation. However, only long CNTs induced IL-1α secretion.[46, 47] Interestingly, when phagocytosis was inhibited by blocking K^+ efflux, IL-1β secretion was suppressed, indicating that phagocytosis is required for inflammasome activation.[46] In general, phagocytosis is the most likely mechanism of entry of CNTs into cells. However, CNTs have also been localized in many non-phagocytic cells where intracellular entry takes place possibly via direct penetration or needling.[43, 48] CNT-endocytosis can be mediated by scavenger receptor, which requires absorption of albumin or other serum proteins.[49] The immune cells can also respond to the presence of CNTs by producing pro-as well as anti-inflammatory cytokines, which can alter innate and adaptive immune responses. Multiple-walled CNTs (MWCNTs) have been shown to stimulate secretion of pro-inflammatory cytokines such as IL-1β, TNF-α, IL-8 and IL-6.[36, 42, 43] Aerosolized pristine single-walled CNTs (SWNTs) have been shown to induce an acute and robust inflammatory response *in vitro*[46] and *in vivo*.[50] Recently, we showed that several types of pristine and non-covalently functionalized CNTs activate the complement system up to C3 and C5, confirming that the entire complement system is activated. Complement activation and deposition on the surface of these CNTs enhanced their uptake by a macrophage (U937) cell line and human monocytes in a time-dependent manner. Complement opsonization of CNTs also led to modulation (mostly down-regulation) of pro-inflammatory cytokine production.[28]

In this study, three different nanoparticles are examined: two functionalized CNTs and a PEGylated gold coated nickel (PEG-Au–Ni) nanowire of similar dimensions to the CNTs. Gold nanoparticles are highly desirable in nanomedicine.[51, 52] However, little is known about their interactions with the immune system. Dobrovolskaia et al.[53] showed that C3 is able to bind to gold nanoparticles, but without activating complement.[51] Most gold nanoparticles are spherical or rod-like. However, here we used wire-like particles to ensure that shape induced responses are similar for the gold and carbon-based nanoparticles. We also examined whether complement deposition, or lack of it, can disrupt innate-adaptive axis via modulation of regulatory cytokines. Thus, carboxymethyl cellulose (CMC) coated CNTs (CMC-CNT), RNA coated CNTs (RNA-CNTs), and Au–Ni nanowires were challenged against U937 (a monocytic cell line derived from histiocytic lymphoma), Raji (a B cell line derived from Burkitts lymphoma) and Jurkat (a T cell line derived from acute T cell leukemia) cells with and without complement deposition. Our results suggest that complement deposition on CNTs determines the balance between pro-inflammatory and anti-inflammatory responses by immune cells. Au–Ni nanowires were poor

inducers of complement activation, and were not pro-inflammatory. However, lack of complement deposition shifted that balance towards inflammatory response following treatment with human serum. On the other hand, complement deposition sequestered CNTs towards a non-inflammatory uptake by immune cells that express complement receptors on their surfaces, such as macrophages and B lymphocytes. Consequently, complement deposition also altered IL-10 and IL-12 cytokine profile, which is likely to raise the threshold of the adaptive immune response. In addition, massive up-regulation of IL-10 is a likely mechanism for the down-regulation of pro-inflammatory cytokines by complement-opsonized nanoparticles. These results have implications when considering the requirements needed for the systemic and direct-to-organ/tissue delivery of the nanoparticles in general.

MATERIALS AND METHODS

Nanoparticles

MWNTs were prepared as described earlier.[54] CNTs were dispersed using non-covalent functionalization via 2 min ultrasonication in PBS containing 1% CMC cellulose (Sigma), or 1% (w/v) RNA from baker's yeast (Sigma). Excess surfactant was removed by washing with PBS. PEG-Au–Ni nanowires, prepared by electrodeposition and fully characterized,[55] were coated with 9 mM glutathione and 1 mM mPEG-SH (Rapp Polymere, Germany) in PBS for 24 h at 4 °C. Excess surfactant was removed by washing in PBS via centrifugation. The nanoparticles were analyzed using a Zeiss HR-LEO 1550 FEG Scanning Electron Microscope (SEM) (Fig. 1). Dispersed nanoparticle samples were deposited on silicon wafers, excess material was blotted, and the wafers were allowed to dry overnight.

The full quality control and characterization of all the nanoparticles used in this study have been reported earlier.[54, 55] The batch consistency in terms of size, purity, absence of debris and contaminations (e.g., catalyst particles) was tested by extensive SEM imaging. Representative images in Figure 1 show no indications of debris and catalyst impurities. After coating with RNA or CMC, CNTs were well-dispersed and relatively monodisperse (length 2.8 ± 0.5 μm, diameter 42 ± 8 nm). The excess dispersants were removed (analysed by OD260 measurements for RNA) and no present carbon film was visible on SEM and TEM images (not presented). PEG-Au–Ni nanowires were fully coated with Au, had a smooth surface without any impurities or other particles present, and were highly monodisperse (length 2.6 ± 0.3 μm, diameter 150 nm). The particles could be properly dispersed in cell media (analyzed by microscopy).

Complement Assays for the Classical and the Alternative Pathways

Briefly, nanoparticle suspensions (100 μl of 100 μg/ml stock) in PBS were added to 100 μl of fresh human serum diluted 1:1 in dextrose gelatin veronal buffer with Mg^{2+} and Ca^{2+} ($DGVB^{++}$). Zymosan (0.2 mg in 100 μl PBS; Sigma) served as a positive control, while PBS alone was used as a negative control. To avoid possible interference of the nanoparticles with the assay, the samples were centrifuged (13000 g, 10 min) after 1 h incubation at 37 °C, removing all particles with bound complement factors from the sera. The remaining complement activity of the supernatants of each sample was determined. The supernatants were serially diluted 2-fold (1/10-1/5120 in $DGVB^{++}$) using a 96 well plate. Then, 100 μl of each dilution was incubated with 100 μl of antibody (hemolysin) sensitized sheep erythrocytes (EA) (TCS, Buckingham, UK) as described previously[22] at the concentration of 10^8 cells/ml in $DGVB^{++}$ for 1 h at 37 °C. After incubation, cells were spun down (700 g, 10 min, RT), and released hemoglobin was measured at 541 nm

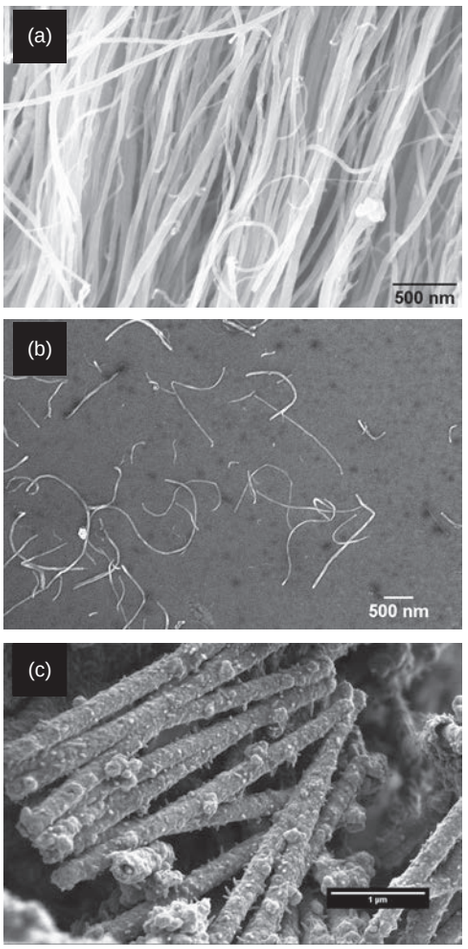

Figure 1. SEM image of (a) pristine MWNTs; (b) CMC-coated and dispersed MWNTs (CMC-CNTs); and (c) Au coated Ni nanowires, dispersed by coating with glutathione and SH-PEG (PEG-Au–Ni nanowires). Samples for SEM were dispersed in water, deposited on silicon wafer, and then blotted after several seconds to allow adherence of the nanoparticles to the surface.

using the supernatant. Total hemolysis (100%) was measured by lysing EA with water. Background spontaneous hemolysis (0%) was determined by incubating EA with buffer only. Hemolytic complement (CH50) values, the serum dilution required for 50% cell lysis, were calculated and compared.

For the alternative pathway assay,[22] nanoparticle suspensions (100 μl of 100 μg/ml) in PBS were added to 100 μl undiluted human serum. Zymosan was used as a positive control. After 1 h of incubation at 37 °C, the nanoparticles were removed by centrifugation (13000 g, 10 min). The supernatants of each sample were serially diluted 2-fold (1/5-1/320) in DGVB-Mg-EGTA placed in 96 well plates. This buffer was used to inhibit complement activation through the classical and the lectin pathways in the absence of Ca^{2+}. 100 μl of each dilution was incubated with 100 μl of antibody sensitized rabbit erythrocytes (10^9 cells/ml in DGVB-Mg-EGTA) for 1 h at 37 °C.

Although the nanoparticles were removed from the sera, control experiments were performed by incubating the CNTs with rabbit and sheep red blood cells for 2 h at 37 °C. No hemolysis was observed in these samples.

Phagocytosis Assay

In order to quantify the CNTs taken up by the immune cells, the nanoparticles were labeled with biotin. In a previous study, no variations in cytokine expression by U937 and monocytes were observed when challenged with labeled and unlabeled CNTs.[28] CMC-CNTs were dialysed against 0.1 M MES buffer and the concentration was adjusted to 0.2 mg/ml. Pentylamine biotin (Pierce) (10 mg) was added to 10 ml of CMC-CNT and 100 μl of a solution of 1-Ethyl-3-(3-dimethylaminopropyl)carbodiimide (EDC) (20 mg/ml; Pierce) was added and stirred for 2 h at RT. The reaction was stopped by adding 100 μl of 0.1 M ethanolamine, and then dialysed against PBS overnight. Stability of the biotin was analysed by incubating the CNTs overnight in various cell culture media (PBS; DMEM with and without 10% FCS). CNTs were removed by centrifugation and supernatant was collected. No biotin could be detected in the supernatants.

U937, Raji and Jurkat cell lines were cultured in complete RPMI containing 10% FCS, 2 mM L-glutamine, 100 U/ml penicillin, 100 μg/ml streptomycin, and 1 mM sodium pyruvate. In a 24 well plate, 5×10^5 cells were incubated in either complete RPMI, or AIM-V AlbuMAX serum-free medium (GIBCO) containing the above supplements. All experiments were performed in duplicates. Biotinylated-CMC-CNTs (20 μg) were added to each well and incubated for 15, 30, 45, 60, 120 or 360 min. Control experiments were performed using cells and PBS only. Cells were harvested and washed five times in PBS via centrifugation at 300× g. After removing supernatants, 25 μl lysis buffer (10 mM HEPES, 20 mM NaCl, 0.5 mM EDTA, 1% w/v Triton X-100) was added to the cells. After lysing the cells, 25 μl of 0.1 mg/ml horse IgG (used as a blocking agent) in PBS was added to the dispersion for further quantification.

A fully calibrated ELISA was used to quantify the amount of CNTs taken up by immune cells.[28] Briefly, microtitre wells (NUNC, polysorb) were coated with 100 μl Avidin (Pierce) (50 μg/ml concentration solution) in 0.1 M sodium carbonate/bicarbonate, pH 9.6 overnight at 4 °C. This was followed by blocking with 1 mg/ml horse IgG for 1 h at RT. Next, 50 μl of a solution or cell lysate containing biotinylated-CMC-CNTs and 50 μl of 0.1 mg/ml horse IgG in PBS were incubated together for 1 h. The microtitre wells were washed 7 times with horse IgG solution to remove excess CNTs and then incubated with 1:2000 Streptavidin-HRP (Sigma) for 1 h at RT. Following washing again, O-Phenylenediamine dihydrochloride (Sigma-Aldrich) was used as a substrate and the yellow 2,3-Diaminophenazine product was measured at 450 nm.

Preparation of Macrophages and Fluorescence Microscopy

The uptake of biotinylated as well as fluorescently-labeled CMC-CNTs following serum treatment, was examined microscopically using monocyte-derived human macrophages. Human peripheral blood mononuclear cells (PBMCs) containing monocytes were obtained by separating heparinized human blood on Ficol-Paque (GE Healthcare) density gradient according to the manufacturer's instruction. The PBMC were then re-suspended at a concentration of 0.5×10^6 cells per ml in complete medium (RPMI, 2 mM L-glutamine, 100 μg/ml Penicillin/Streptomycin and 10% FCS). 1×10^6 PBMCs were seeded on 13 mM diameter cover slips and incubated for 7 days at 37 °C in 5% CO_2 in a humidified atmosphere. Mature macrophages were separated from non-adherent cells by washing with sterile PBS before the experiments.

CMC-CNTs were re-suspended in 0.1 M MES buffer (2-(*N*-morpholino)ethanesulfonic acid, pH 5.0) and labeled with AlexaFluor488-cadaverine for 2 h at RT in a 2:1 ratio (CNT:label) in the presence of 1 mM EDC. Labeled CMC-CNTs were recovered by centrifugation at 10,000 g for 10 min. Normal human serum treatment of biotinylated and fluorescently labeled CMC-CNTs was carried out for 1 h at 37 °C with agitation. Excess serum was removed by washing twice with PBS. Complement deposited CMC-CNTs were recovered by centrifugation and dispersed in a water bath sonicator. Macrophages on coverslips were exposed to serum treated and untreated CMC-CNTs in 500 μl of serum-free medium for 3 h at 37 °C in a CO_2 incubator. Cells were then washed twice with PBS, fixed with 4% formaldehyde for 10 min, and then permeabilized in the case of biotinylated CMC-CNTs using permeabilizing buffer (20 mM HEPES-NaOH pH 7.4,

300 mM sucrose, 50 mM sodium chloride, 3 mM magnesium chloride, 0.5% Triton X-100, 0.1 M sodium azide in 1 ml H_2O) for 5 min on ice. Fluorescently-labeled CMC-CNTs were directly processed for immunofluorescence without permeabilization. The coverslips were blocked using 5% FCS in PBS for 30 min and stained for 30 min with Hoechst 33342, AlexaFluor488-phalloidin and AlexaFluor546-labeled streptavidin (in the case of biotinylated CMC-CNTs). Cells, incubated with fluorescently labeled CMC-CNTs, were stained with 2 μg/ml AlexaFluor546-conjugated Wheat Germ Agglutinin for 30 min. Cells were then washed and observed with an Olympus fluorescence microscope using SmartCapture 3 imaging software, or a Zeiss 780 confocal microscope with 40× oil lens using ZEN software.

Measurement of Cytokine Expression Using Real-Time Quantitative PCR Analysis

To a 24 well cell culture plate containing 5×10^5 U937, Raji or Jurkat cells, 20 μg of CMC-CNTs, RNA-CNTs, or PEG-Au–Ni nanowires in PBS were added and incubated for 15, 30, 45, 60, 120 or 360 min. Control experiments were performed by incubating cells with PBS instead of nanoparticle suspensions. Cells were harvested (3000 g, 5 min) and total RNA was extracted using the GenElute Mammalian Total RNA Purification Kit (Sigma-Aldrich). Any contaminating DNA was removed by DNase I treatment (Sigma-Aldrich), followed by heat-inactivation of DNase I. The amount of total RNA was determined at 260nm using NanoDrop 2000/2000c (Thermo-Fisher Scientific), and the purity was assessed using 260/280 nm ratio. cDNA was synthesized using High Capacity RNA to cDNA Kit (Applied Biosystems) using 2 μg of total RNA.

Primers were designed using Primer-BLAST software (http://blast.ncbi.nlm.nih.gov/Blast.cgi). These were: 18S forward (5′-ATGGCCGTTCTTAGTTGGTG-3′), 18S reverse (5′-CGCTGAGCCAGTCAGTGTAG-3′); IL-1β forward (5′-GGACAAGCTGAGGAAGATGC-3′), IL-1β reverse (5′-TCGTTATCCCATGTGTCGAA-3′); IL-6 forward (5′-GAAAGCAGCAAAGAGGCACT-3′), IL-6 reverse (5′-TTTCACCAGGCAAGTCTCCT-3′); IL-10 forward (5′-TTACCTGGAGGAGGTGATGC-3′), IL-10 reverse (5′-GGCCTTGCTCTTGTTTTCAC-3′); IL-12 forward (5′-AACTTGCAGCTGAAGCCATT-3′), IL-12 reverse (5′-GACCTGAACGCAGAATGTCA-3′); TGF-β forward (5′-GTACCTGAACCCGTGTTGCT-3′), TGF-β reverse (5′-GTATCGCCAGGAATTGTTGC-3′); and TNF-α forward (5′-AGCCCATGTTGTAGCAAACC-3′), TNF-α reverse (5′-TGAGGTACAGGCCCTCTGAT-3′).

The qPCR reaction included 5 μl Power SYBR Green MasterMix (Applied Biosystems), 75 nm forward and reverse primers and 500 ng template cDNA in a 10 μl reaction volume. PCR was performed using the Step One Plus Real-Time PCR System (Applied Biosystems). After initiation steps of 2 min at 50 °C and 10 min at 95 °C, the template was amplified for 40 cycles, each cycle comprised of 15 sec at 95 °C and 1 min at 60 °C. Samples were normalized using the expression of human 18S rRNA. Data was analyzed using the Step One software v2.3 (Applied Biosystems). Ct (cycle threshold) values for each cytokine gene were calculated. Relative expression of each cytokine gene was calculated using the Relative Quantification (RQ) value, using the equation: $RQ = 2^{-\Delta\Delta Ct}$ for each cytokine gene, and comparing relative expression with that of the 18S rRNA constitutive gene product. Experiments were conducted in triplicate.

Multiplex Cytokine Array Analysis

Cytokines (IL-1α, IL-1β, IL-6, IL-8, IL-10, TNF-α) and chemokines/growth factor (MCP-1, VEGF, GM-CSF and GRO) concentrations in the supernatant of the cell culture experiments were measured by MagPix Milliplex kit (EMD Millipore). Briefly, 25 μl of assay buffer was added to each well of a 96-well plate. This was followed by addition of 25 μl of standard, controls or supernatants of immune cells treated for 12, 24 or 48 h with CMC-CNTs, RNA-CNTs or PEG-Au–Ni nanowires, to appropriate wells. 25 μl of magnetic beads coupled to analytes of interest were added in each well, followed by incubation for 18 h at 4 °C. The 96-well plate was washed with assay buffer and 25 μl of detection antibodies were incubated with the beads for 1 h at RT. 25 μl of Streptavidin-Phycoerythrin conjugate was then added and incubated for 30 minutes. Following a washing step, 150 μl of sheath

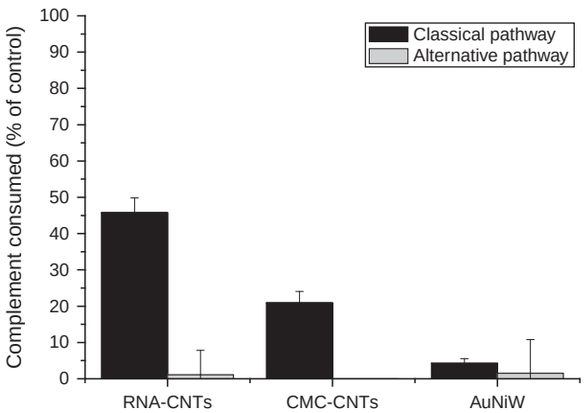

Figure 2. Complement activation by RNA-CNTs, CMC-CNTs and PEG-Au–Ni nanowires. Nanoparticles were incubated with serum at 37 °C. After 1 h, the nanoparticles were removed by centrifugation and the supernatants were tested for the presence of complement proteins and complement activity using hemolytic assays. Positive controls were incubated with Zymosan, whereas negative control samples with PBS only. Complement activity of the samples was compared to the negative control and depleted complement was calculated from the results. Experiments were performed in triplicate. Error bars indicate standard deviations.

fluid was added to each well and the plate was read using the Luminex Magpix instrument.

Statistical Analysis

Statistical analysis was performed using GraphPad Prism version 6.0 (GraphPad Software). A 2-way ANOVA test was used to compare the mean of the cytokine targets between serum and no serum conditions for any significant differences in gene expression, at various time-points. *P* values were computed, and graphs were compiled and analyzed.

RESULTS

PEG-Au–Ni Nanowires Very Weakly Activate the Classical and the Alternative Pathways Compared to the CMC- and RNA-CNTs

All CNT samples tested activated complement through the classical pathway and negligibly by the alternative pathway. PEG-Au–Ni nanowires showed negligible complement activation (Fig. 2). RNA-CNTs were nearly 2 times better complement activators than the CMC-CNTs as far as the classical pathway was concerned.

Cell Lines Expressing Complement Receptors (U937, Raji and Macrophages) Show Enhanced Uptake of CMC-CNTs Following Serum Treatment

Cellular uptake of complement-activating CMC-CNT was studied via an ELISA method using three different cell lines. Uptake of CMC-CNTs, primarily seen in macrophages (U937) and B (Raji) cells and, to a lesser extent, in Jurkat T cells, was time-dependent and took place essentially over the first 45 min (Fig. 3). Subsequently, fluorescence and confocal microscopy were used to examine uptake of CMC-CNTs by human macrophages. Figures 3(b) to (e) demonstrate that serum treatment enhances uptake of CMC-CNTs independent of the functional group that has been attached. Both Alexa488 cadaverine-labeled as well as biotin-labeled CMC-CNTs were endocytosed more efficiently after serum treatment. Adherence of the CNTs to the cells was not affected

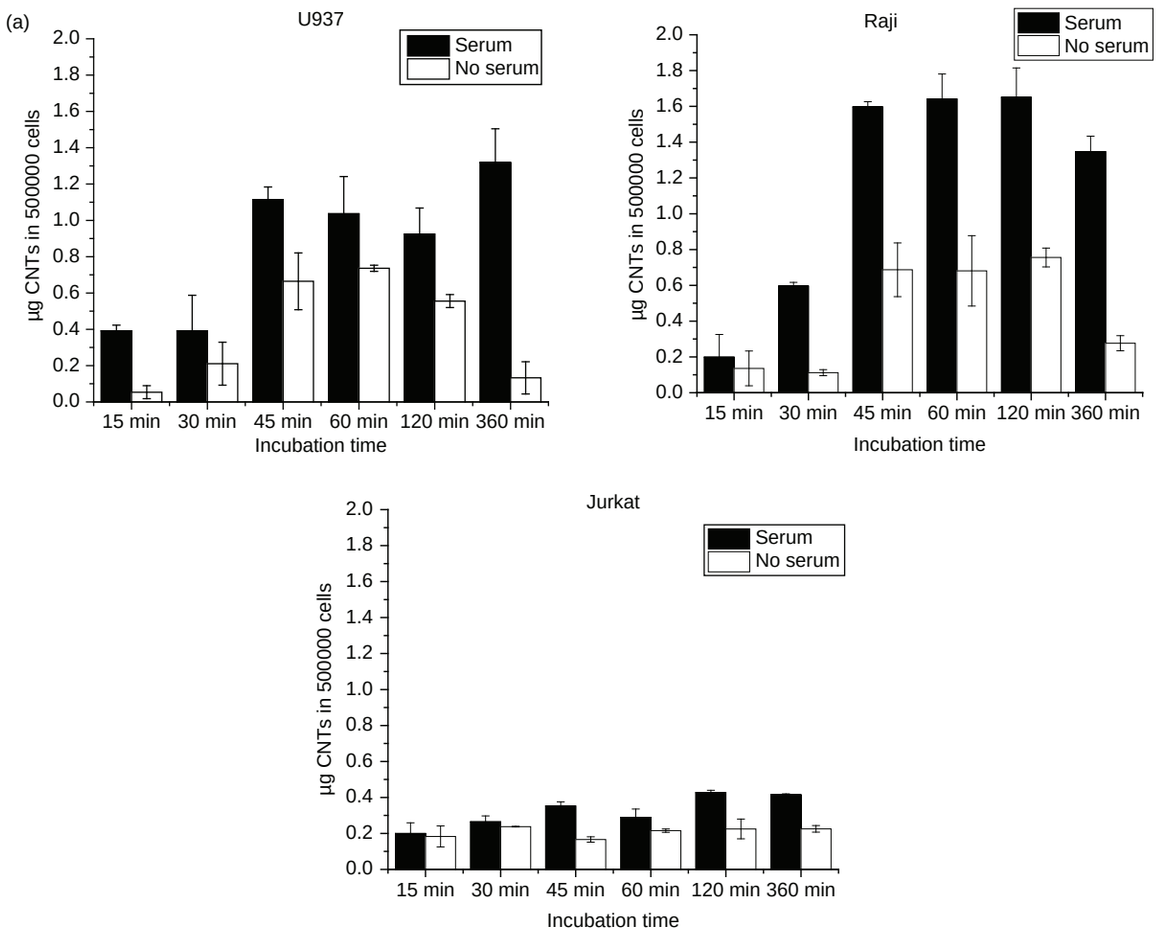

Figure 3. Continued.

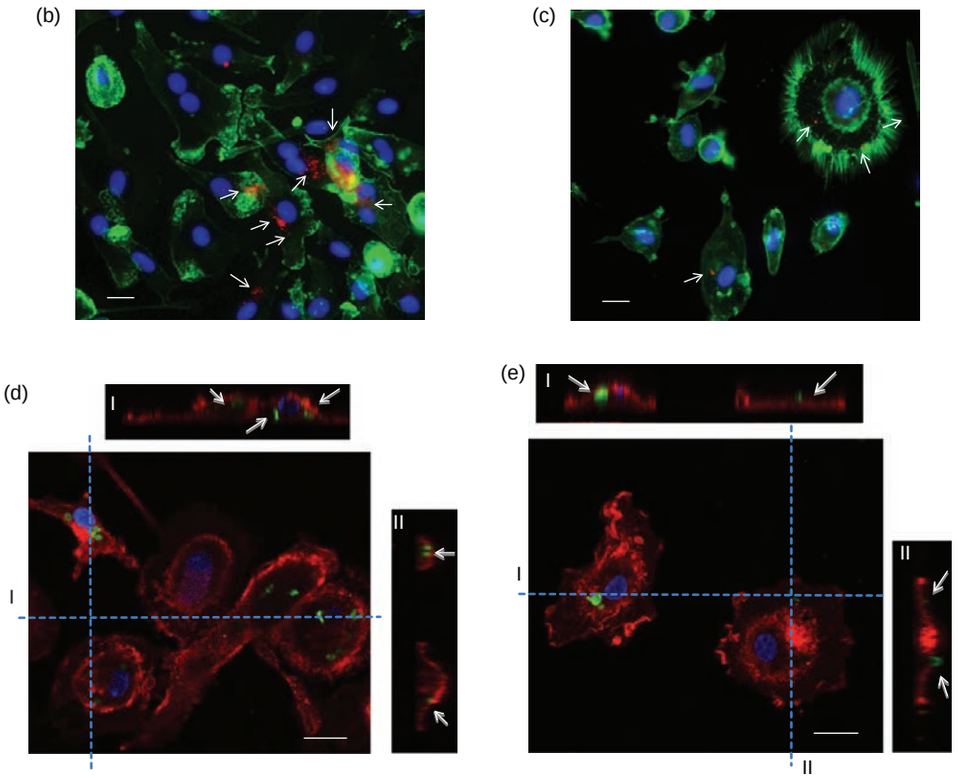

Figure 3. **(a) *In vitro* assessment of the uptake of serum treated and untreated biotinylated CMC-CNTs by various cell types analysed by an ELISA based procedure. Uptake of CNTs was analysed using U937, Raji and Jurkat cells. Jurkat T cells showed little uptake whereas U937 and Raji cells showed greater uptake of CNTs. In each case, serum-treatment of CNTs enhanced pahgocytosis. To confirm the results, microscopy was performed to show uptake of serum-treated and untreated biotinylated CMC-CNTs by human blood macrophages. Cells were incubated with serum-treated (b) and untreated biotinylated CMC-MWCNTs (c) for 3 h. Cells were fixed, permeabilized and stained for filamentous actin (green). The nucleus was revealed with Hoechst 33342 (blue) and biotinylated CMC-CNTs were visualized with AlexaFluor546-labelled Streptavidin (red, arrows). Scale bar, 10 μm. To confirm internalization, confocal microscopy was used. Human blood macrophages were incubated with serum-treated (d) and untreated AlexaFluor488 cadaverine-labeled CMC-CNTs for 3 h. (e) (green, arrows in orthogonal views). Cells were fixed and stained with AlexaFluor546-labeled wheat germ agglutinin to reveal the plasma membrane (red). The nucleus was stained with Hoechst 33342 (blue). A confocal section and orthogonal views created at the blue dashed lines indicated with I and II are shown. Scale bars, 20 μm.**

as shown in Figures 3(c) and (e); CNTs untreated with serum could be seen attached to the plasma membrane of human macrophages visualized by staining with Alexa546 labeled Wheat Germ Agglutinin. However, after serum treatment, uptake of CNTs was observed (Figs. 3(c) and (d)). This finding is in agreement with an earlier study that reported stimulation of MWNT uptake by normal human bronchial epithelial cells following serum treatment.[56]

Complement Deposition on CMC- and RNA-CNTs Prime U937 Cells for Suppression of Pro-Inflammatory Cytokine mRNA Expression

CMC-CNT induced considerable mRNA expression of TGF-β, IL-12, TNF-α and IL-1β by U937 cells within 1 h of challenge compared to the control samples (Fig. 4(a)). Serum-treated CMC-CNTs significantly down-regulated IL-6, IL-10, TNF-α, TGF-β and IL-1β mRNA expression by U937 cells, while suppressing IL-12 slightly in a biphasic manner. Levels of IL-1β, MCP-1, TNF-α and VEGF in the supernatant of U937 cells were lower in the presence of serum-treated CMC-CNTs compared to untreated CMC-CNT. In contrast, IL-10 levels were higher in the case of serum-treated CMC-CNT. In the case of RNA-CNT, the mRNA expression of IL-10, IL-6, TGF-β, TNF-α and IL-1β was up-regulated without serum, but considerably down-regulated in the presence of serum (Fig. 5(a)). Levels of MCP-1, TNF-α and VEGF in the supernatants were lower for the serum-treated RNA-CNTs (Fig. 7).

Complement-Opsonised CNTs Down-Regulate Pro-Inflammatory Cytokine mRNA Synthesis But Enhance IL-12 Transcripts by the B Cell (Raji) Line

Challenging Raji cells with complement-opsonised CMC-CNTs led to downregulation of IL-6, IL-10, TNF-α and IL-1β transcripts. Curiously, IL-12 mRNA levels were considerably up-regulated by serum treatment, suggesting likely enhancement of antigen presentation and Th1 activation leading to IFN-γ production (Fig. 4(b)). In the case of RNA-CNTs, IL-10 was consistently up-regulated in the presence of serum, while TGF-β and IL-12 were dramatically up-regulated within 30 min (Fig. 5(b)). IL-1β and TNF-α transcripts were down-regulated by complement deposition (Fig. 5(b)).

Jurkat T Cells Appear to Respond Feebly in Terms of Cytokine Production When Challenged with CNTs With or Without Serum

Consistent with poor uptake of CNTs (Fig. 3(a)), Jurkat T cells were weak responders in terms of cytokine mRNA synthesis (Figs. 4(c), 5(c), 6(c)). In the case of CMC-CNTs, Jurkat cells produced very little cytokine mRNA expression, which was further suppressed in the presence of serum (with the exception of IL-12) (Fig. 4(a)). In the case of RNA-CNTs, most cytokine transcripts were expressed at a very low level (Figs. 5(a)–(c)).

Lack of Complement Activation by PEG-Au–Ni Nanowires Exaggerates Pro-Inflammatory Cytokine mRNA Synthesis

PEG-Au–Ni nanowires, in general, produced feeble effects on the three cell lines tested (Fig. 6). However, the serum treatment up-regulated IL-10, TNF-α and IL-1β mRNA expression significantly within 30 min of the challenge (Fig. 6). More interestingly, the transcriptional expression of IL-10, TGF-β, IL-12, IL-6, TNF-α, and IL-1β was dramatically up-regulated when Raji cells were challenged with serum-treated Au–Ni nanowires (Figs. 6(a), (b)).

Multiplex Cytokine Array Analysis Reveals Differential Ability of CNTs and Nanowires to Trigger Regulatory Cytokines by the U937 Cells in a Complement-Dependent Manner

To assess the cytokine biosynthesis and secretion over a period of 48 h, a multiplex cytokine array was used. CMC-CNTs induced massive upregulation of GM-CSF in the U937 cells by 24 h, which declined by 48 h. However, when compared to CMC-CNTs, RNA-CNTs and PEG-Au–Ni induced poor GM-CSF responses. In the case of CMC-CNT, complement deposition (serum-treated) up-regulated GRO, IL-1, IL-8 and IL-10, while GM-CSF, MCP-1, TNF-α and VEGF were down-regulated (Fig. 7). Complement-deposited RNA-CNTs up-regulated GM-CSF, GRO, IL-1β, IL-6 and IL-8, while down-regulating IL-10, MCP-1, TNF-α and VEGF. PEG-Au–Ni nanowires, on its own, up-regulated IL-2α, IL-10 and MCP-1, while being a poor inducer of TNF-α. Serum-treated PEG-Au–Ni nanowires up-regulated GM-CSF, GRO, IL-1β, IL-6 and IL-8 while down-regulating IL-2α (Fig. 7). Thus, PEG-Au–Ni nanowires were good inducers of IL-10 and poor inducers of TNF-α and IL-1β.

DISCUSSION

Recently, we have shown that several types of pristine and non-covalently functionalized CNTs activate the complement system predominantly via the classical pathway until MAC formation.[28] C1q interacts with these CNTs via its ligand-binding globular head domain. CNTs, when opsonized with the recombinant forms of globular head modules, suppressed the classical pathway activation by acting as a competitive inhibitor of serum C1q. Complement deposition on the surface of these CNTs enhanced their uptake by U937 cell line and human monocytes. A significant dampening of pro-inflammatory cytokine response was observed when serum-treated CNTs were challenged to U937 cells.[28] This novel link between complement deposition on CNTs and cytokine response prompted us to examine complement-activating and non-activating nanoparticles and subsequent modulation of immune response by the cells of innate and adaptive immunity. Addressing this question became pertinent since the cytokine signatures of the innate immune response can shape and orient the adaptive immunity. Thus, we set out to examine if complement deposition on CNTs can influence the uptake and subsequent expression of cytokines by U937 macrophages and Raji B cells. Both cell lines express abundant complement receptors and are capable of antigen presentation. In contrast, Jurkat T cells are not phagocytic, express very little complement receptors, and are amenable to modulation by cytokines secreted by macrophages and B cells. In addition to using CMC-CNTs and RNA-CNTs that are complement-activating, PEG-Au–Ni nanowires were also examined since gold nanoparticles are generally not known to activate complement.[53] We show here, for the first time, that PEGylated-gold-coated (PEG-Au–Ni) nanowires do not activate complement significantly through the classical and the alternative pathway. Due to the notable differences in their ability to activate complement by these similarly sized and shaped particles, CMC-CNT, RNA-CNT and PEG-Au–Ni nanowires were considered excellent candidates for clarifying the relationship between complement activation and cytokine production by cell lines representing macrophage, B cell and T cells. Differences in the complement activation by the two types of CNTs might be caused by the degree of coating of the CNTs as well as by the chemical nature of the coating substance. Au–Ni nanoparticles are known to show little complement activation in general.[53] Commonly, small

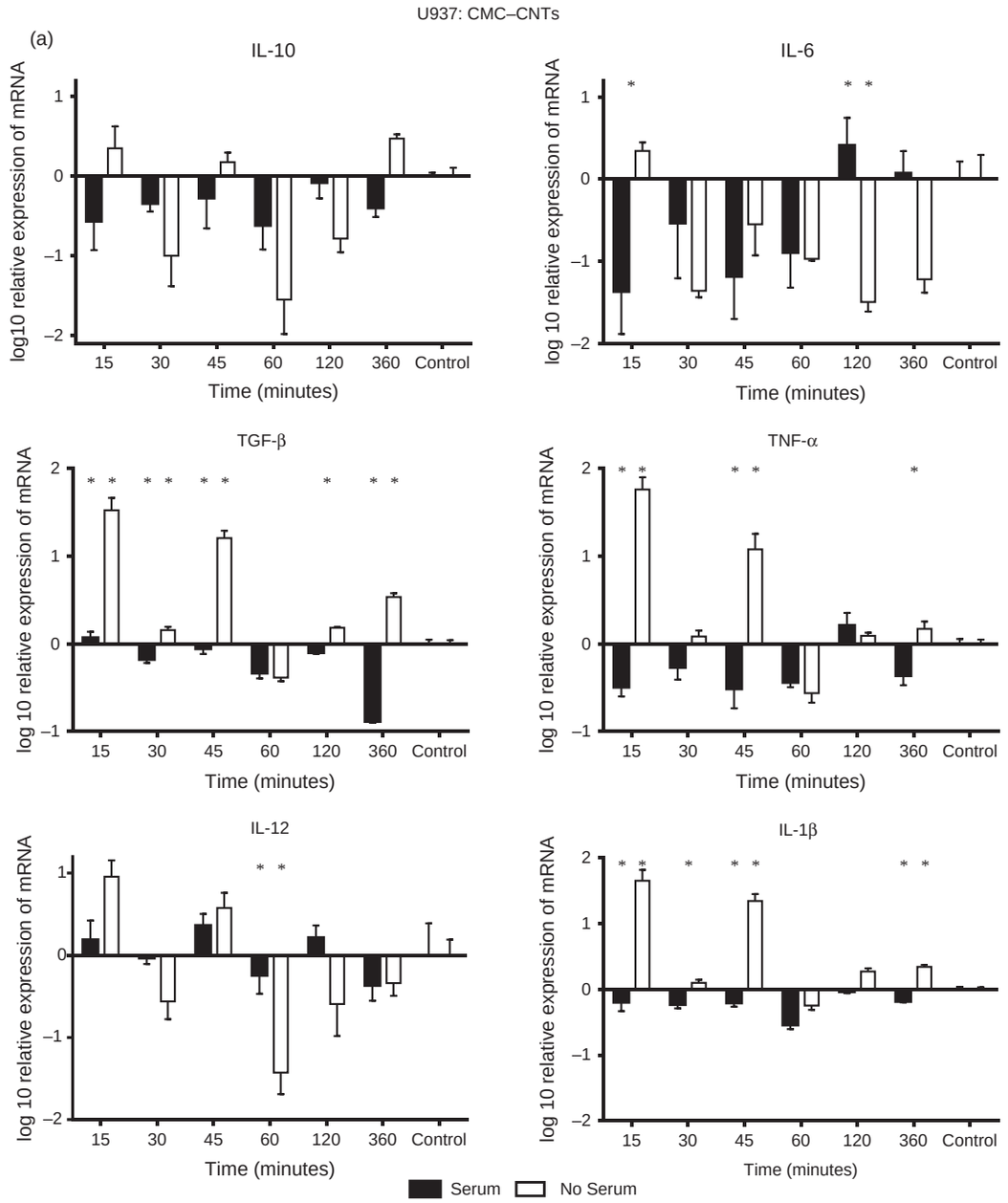

Figure 4. **Continued.**

(3–100 nm) Au nanoparticles are used in biomedical applications, but increasing their dimensions seems to have no effect on their interactions with complement proteins.[51–53]

The phagocytosis of CMC-CNTs by U937 and Raji cells, which are known to over-express complement receptors, was considerably enhanced by serum treatment/complement deposition (Fig. 3). The highest level of phagocytosis of CNTs in the presence of complement-sufficient serum by Raji cells is an indicator of the involvement of complement receptors in the phagocytic process. B cells are known to present the highest number of CD21 and CD35 (CR2 and CR1), which are receptors for iC3b, C3d and C4b, on their cell surface. U937 cells express CR1 as well as the iC3b receptors-CR3 and CR4 (CD11b, CD18; CD11c, CD18). Jurkat cells (like T cells) express very low levels of CD35 and CD11b/CD18,[57] which explains relatively low levels of uptake of CNTs despite serum treatment. In all cases, however, uptake of CMC-CNTs was enhanced in the presence of serum, indicating the importance of complement deposition on the CNTs. The maximum intracellular

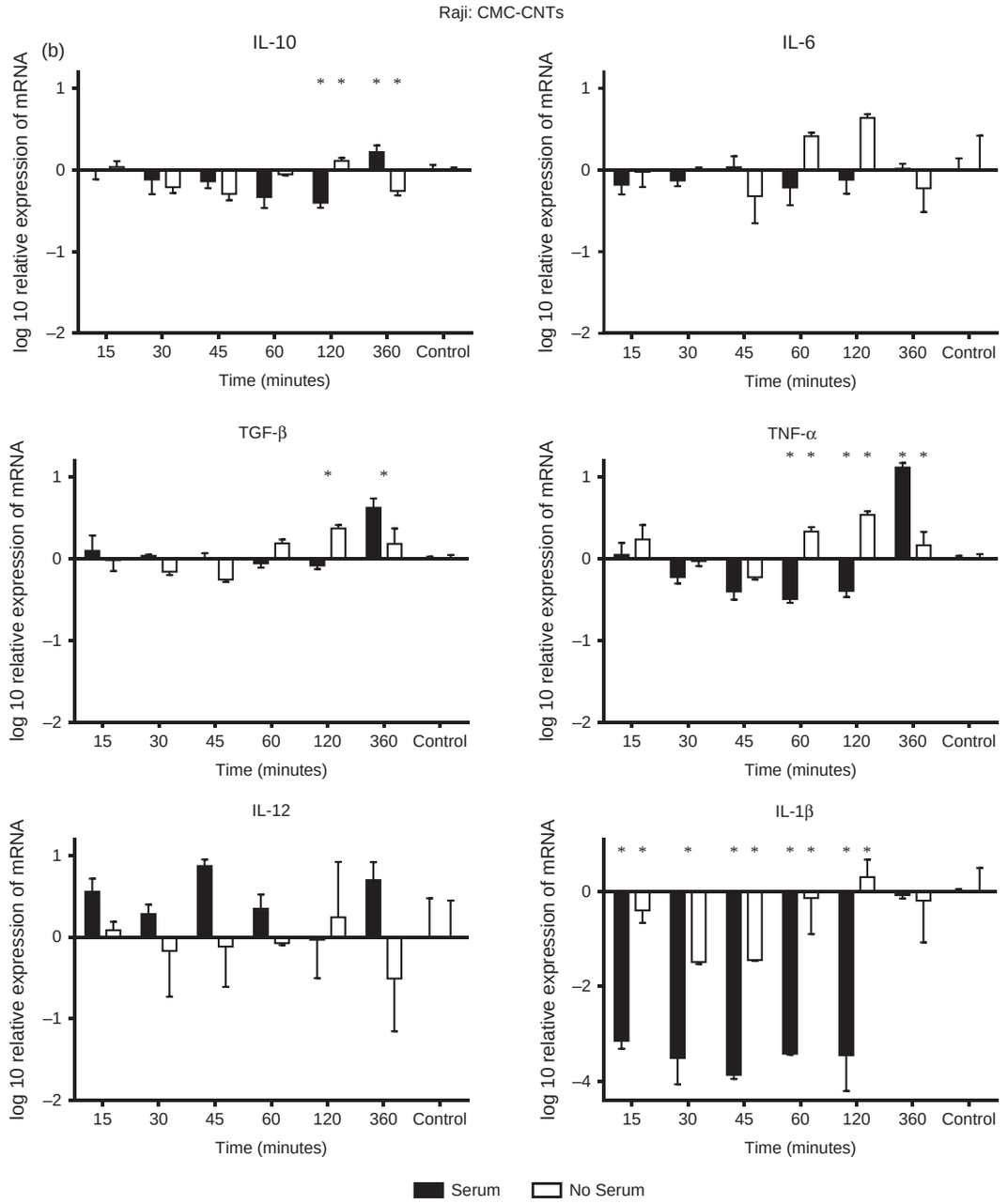

Figure 4. Continued.

CMC-CNTs were detected at 360 and 60 minutes for U937 and Raji cells, respectively, suggesting very rapid turn-over and processing of CNTs by Raji cells. Curiously, CNTs, which were not serum-treated, were less detectable by the 360 minute time-point, suggesting that immune cells were either degrading the coating of non-opsonized CNTs, or discarding them via transcytosis; this is currently being investigated. Complement-opsonized CNTs continued to be detectable inside the cells at least until 360 min after challenge, suggesting that complement deposition may influence the intracellular persistence of CNTs. It is possible that intracellular PRRs such as TLR7 and TLR9 are also able to recognize non-opsonized CNTs, leading up to pro-inflammatory response.

On their own, CMC-CNTs and RNA-CNTs induced very early transcriptional upregulation of pro-inflammatory cytokines TNF-α and IL-1β by U937 cells. Serum treatment significantly down-regulated the expression of these cytokines, in addition to inducing higher IL-10 transcription by CMC-CNTs. Raji cells showed reduced mRNA expression of TNF-α and IL-1β transcripts when

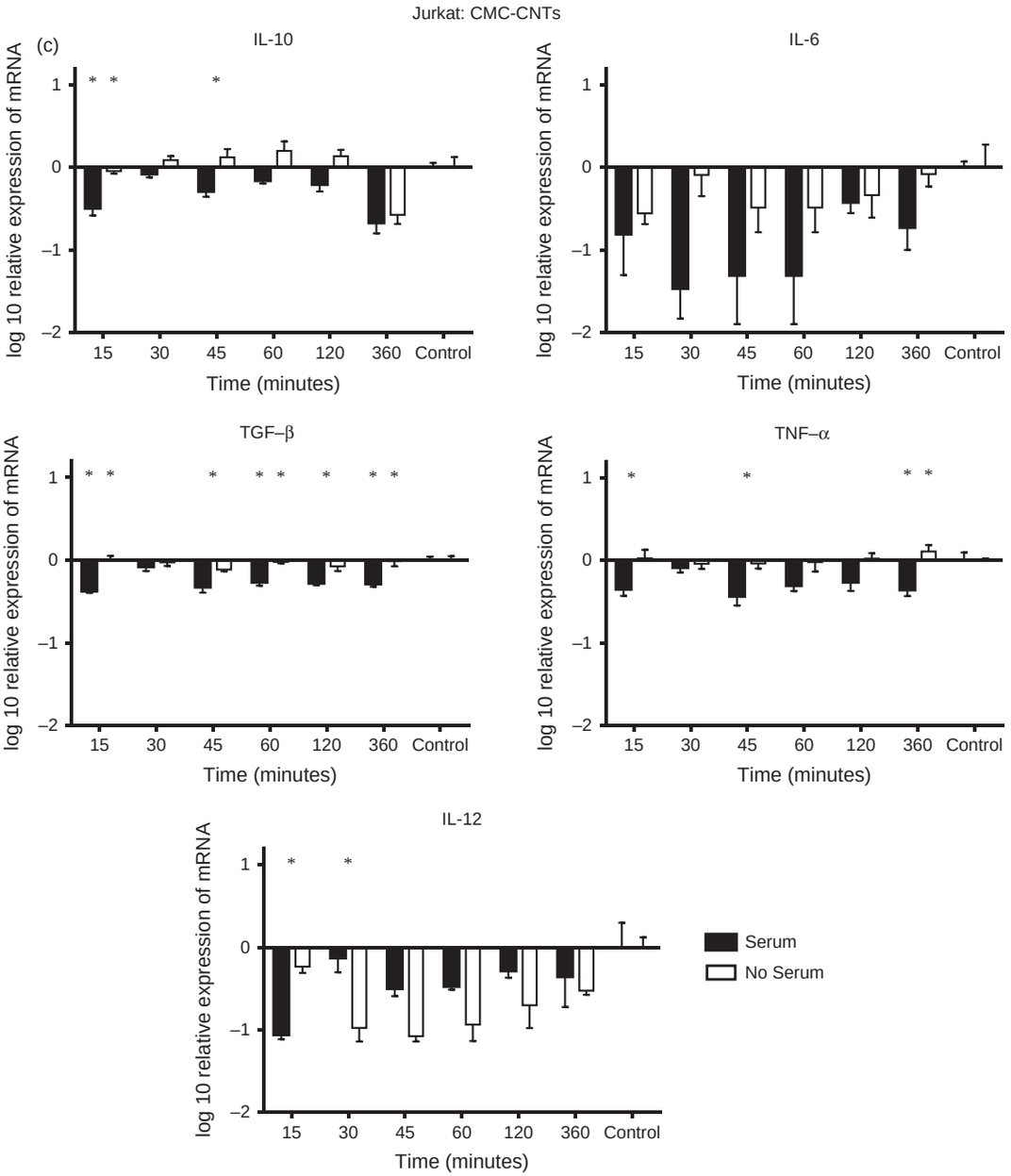

Figure 4. **qPCR analysis of the CMC-CNT induced expression of cytokines by (a) U937, (b) Raji, and (c) Jurkat cell lines. Cells were incubated with CMC-CNTs with prior serum treatment or no treatment at the following time-points: 15, 30, 45, 60, 120 and 360 mins. In control experiments, cells were incubated with PBS only for 30 mins. The expression of cytokine mRNA was measured using real-time qPCR and the data normalized to 18S rRNA gene expression that was used as an endogenous control. Assays were conducted in triplicate. Error bars represent ± standard error of the mean. A 2-way ANOVA was performed on the data to determine significant differences in expression as noted by *: $p \leq 0.05$; **: $p \leq 0.01$).**

challenged by CMC-CNT. For complement-deposited RNA-CNT, IL-10 was consistently up-regulated; TGF-β and IL-12 were dramatically up-regulated; while IL-1β and TNF-α were down-regulated. However, Jurkat T cells were weak immune responders, and whatever little cytokine mRNA expression these cells had was further suppressed by complement deposition on the CNTs. It is clear that T cells are more likely to be modulated indirectly by soluble factors produced by antigen capturing and presenting cells such as macrophages and dendritic cells following interaction with nanoparticles. Complement deposition thus appears

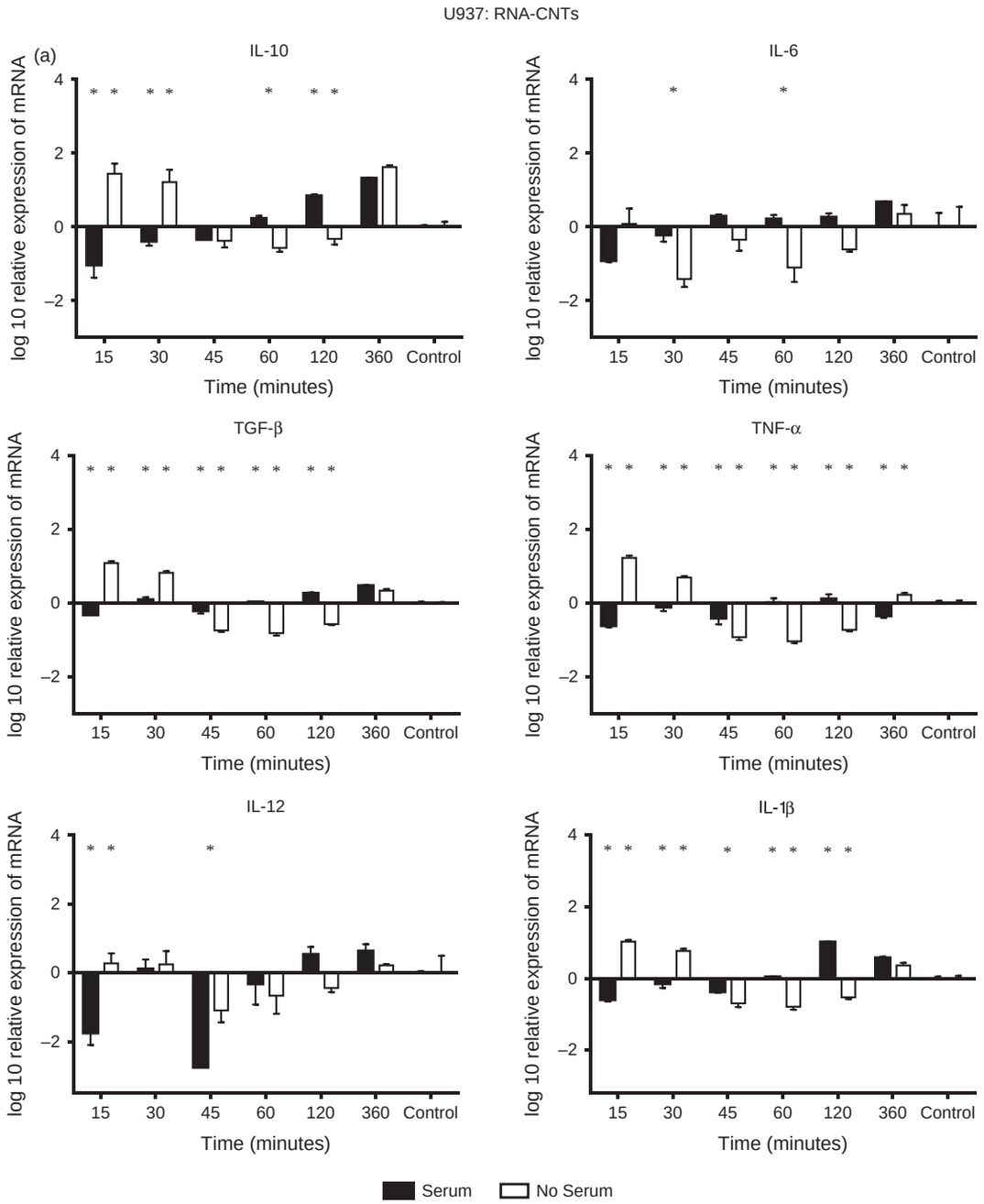

Figure 5. Continued.

to be involved in counterbalancing pro-inflammatory signals arising due to immune cell-nanoparticle interaction. In contrast, PEG-Au–Ni nanowires, which were poor complement activators, enticed a weak transcriptional expression of cytokines tested via qPCR analysis. However, serum-treated PEG-Au–Ni nanowires significantly up-regulated mRNA synthesis of TNF-α and IL-1β by U937 cells. In addition, Raji cells also showed dramatic up-regulation of IL-10, TGF-β, IL-12, IL-6, TNF-α, and IL-1β transcripts, suggesting that some of the serum proteins, other than complement subcomponents, which are known to bind to gold nanoparticles[52] can alter or exaggerate the immune response. A lack of complement deposition on the PEG-Au–Ni nanowires probably offers an opportunity for other serum factors to bind to the surface.

Transcriptional analysis via Real-Time qPCR experiments yields early mRNA synthesis within a few minutes of the cell response to nanoparticles. In order to gauge cytokine secretion over 48 h, a multiplex

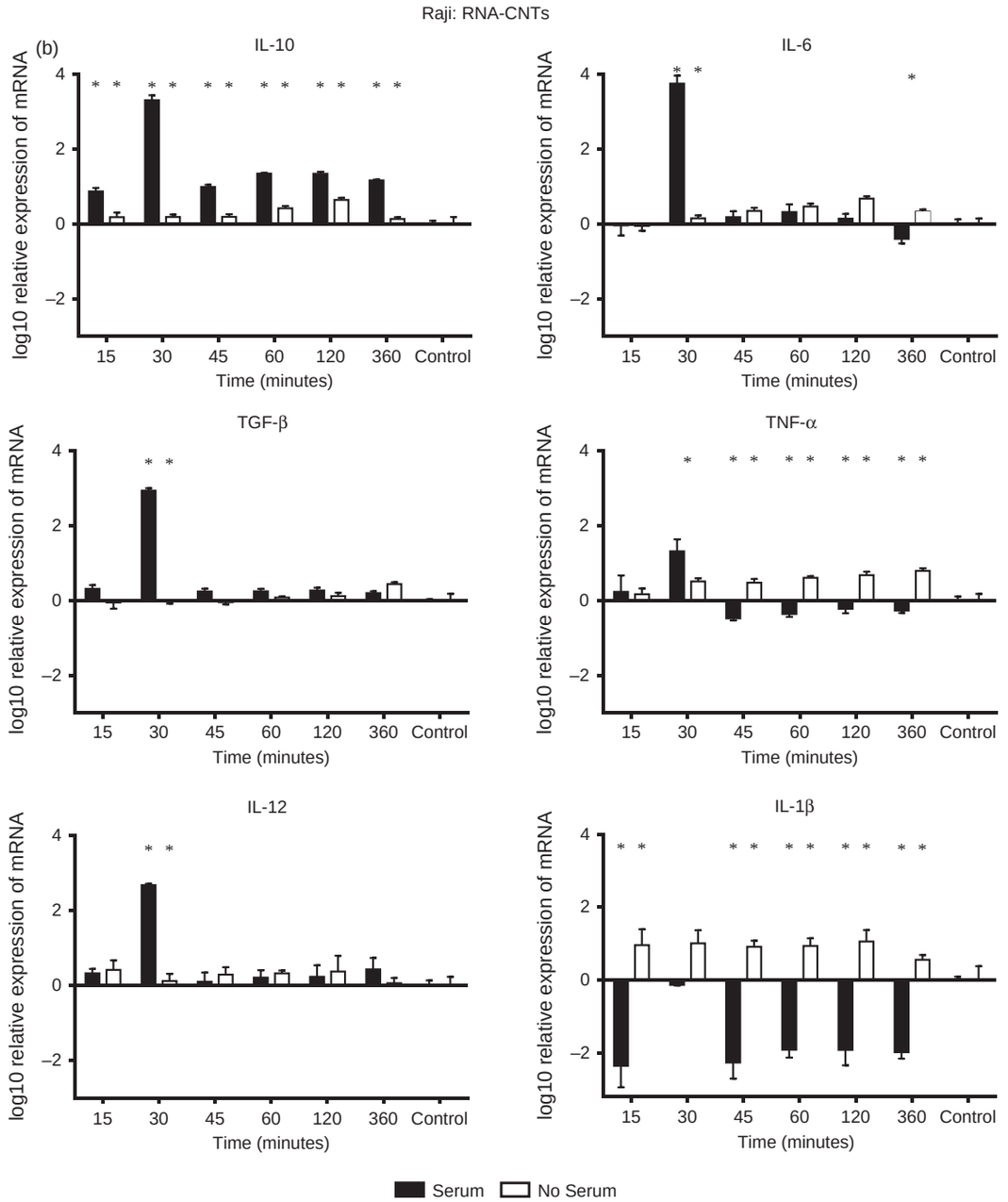

Figure 5. **Continued.**

cytokine array was carried out using supernatants from nanoparticle-challenged immune cells. CMC-CNT induced massive upregulation of pro-inflammatory GM-CSF by all three cell lines by 24 h, which declined by 48 h. However, RNA-CNT and PEG-Au–Ni nanowires induced poor GM-CSF response. GM-CSF is known to be a potent chemotactic factor for neutrophil recruitment. Complement deposition on the CMC-CNTs up-regulated GRO, IL-1, IL-8 and IL-10 while GM-CSF, MCP-1, TNF-α and VEGF were down-regulated. Complement-opsonized RNA-CNTs up-regulated GM-CSF, GRO, IL-1β, IL-6 and IL-8 while down-regulating IL-10, MCP-1, TNF-α and VEGF. PEG-Au–Ni nanowires without serum treatment up-regulated IL-2α, IL-10 and MCP-1 while being a poor inducer of TNF-α. Serum-treated PEG-Au–Ni nanowires up-regulated GM-CSF, GRO, IL-1β, IL-6 and IL-8 while down-regulating IL-2α. Thus, PEG-Au–Ni nanowires were good inducers of IL-10 and poor inducers of TNF-α and IL-1β when they were not treated by serum. This emphasizes the fact that complement

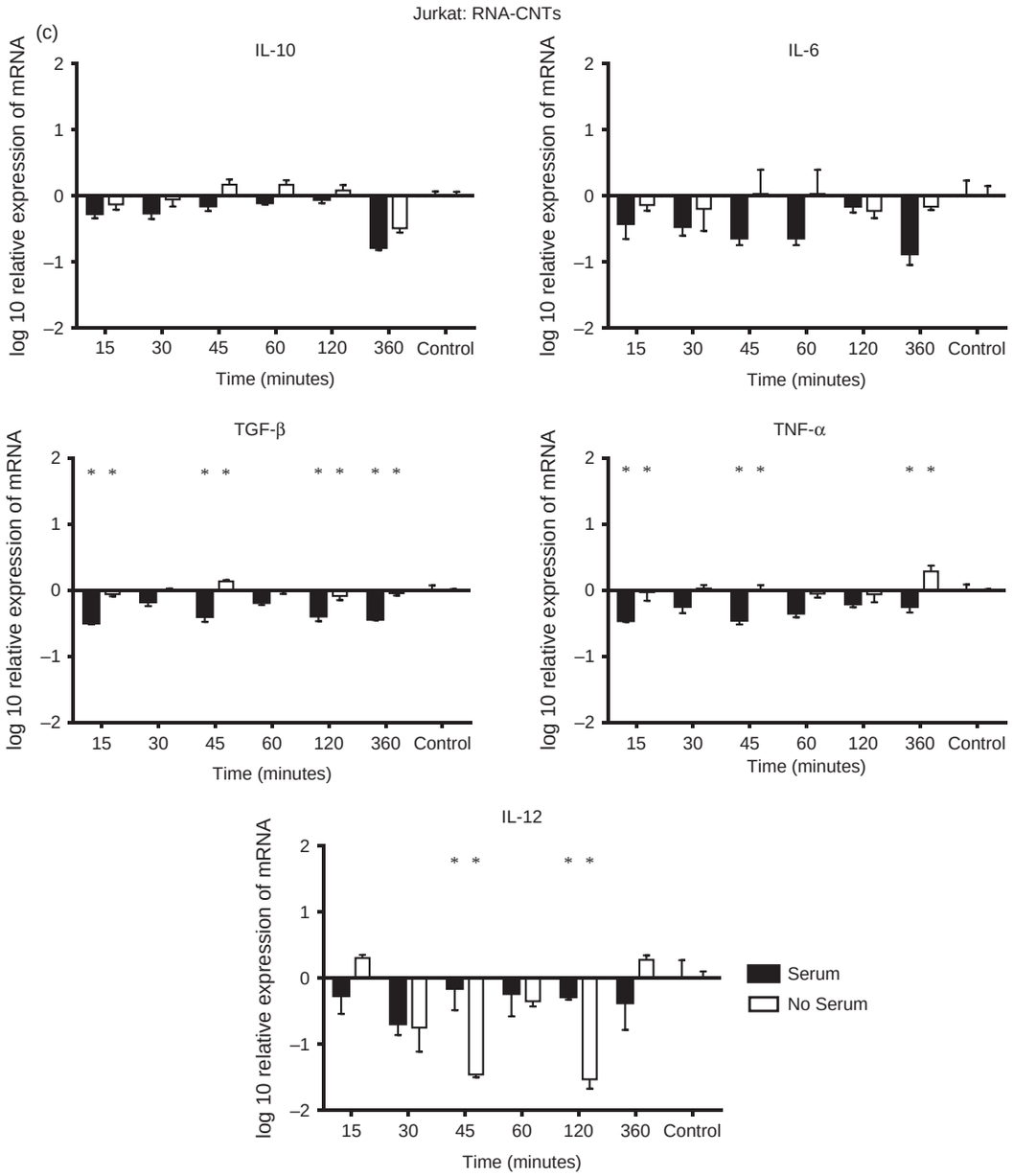

Figure 5. **qPCR analysis of the RNA-CNT induced expression of cytokines by (a) U937, (b) Raji, and (c) Jurkat cell lines. Cells were incubated with RNA-CNTs with serum and without serum treatment at the following time-points: 15, 30, 45, 60, 120 and 360 mins. In control experiments, cells were incubated with PBS only for 30 mins. The expression of cytokines was measured using real-time qPCR and the data was normalized to 18S rRNA gene expression (used as an endogenous control). Assays were conducted in triplicate. Error bars represent ± standard error of the mean. A 2-way ANOVA was performed on the data to determine significant differences in expression as noted by *: $p \leq 0.05$; **: $p \leq 0.01$).**

deposition on the nanoparticles can sequester immune response towards an anti-inflammatory milieu. A lack of complement deposition can render nanoparticles accessible to other serum proteins and soluble factors,[53] which can negate anti-inflammatory effects due to complement opsonization (as is the case here with PEG-Au–Ni nanowires). It is possible that the PEG-Au–Ni nanowires do not offer the necessary charge pattern so that the recognition subcomponents of the complement system do not bind to it and activate the complement cascade.

The suppression of pro-inflammatory cytokines is most likely due to the immunomodulatory effects of IL-10, which through its pleiotropic properties on various cell

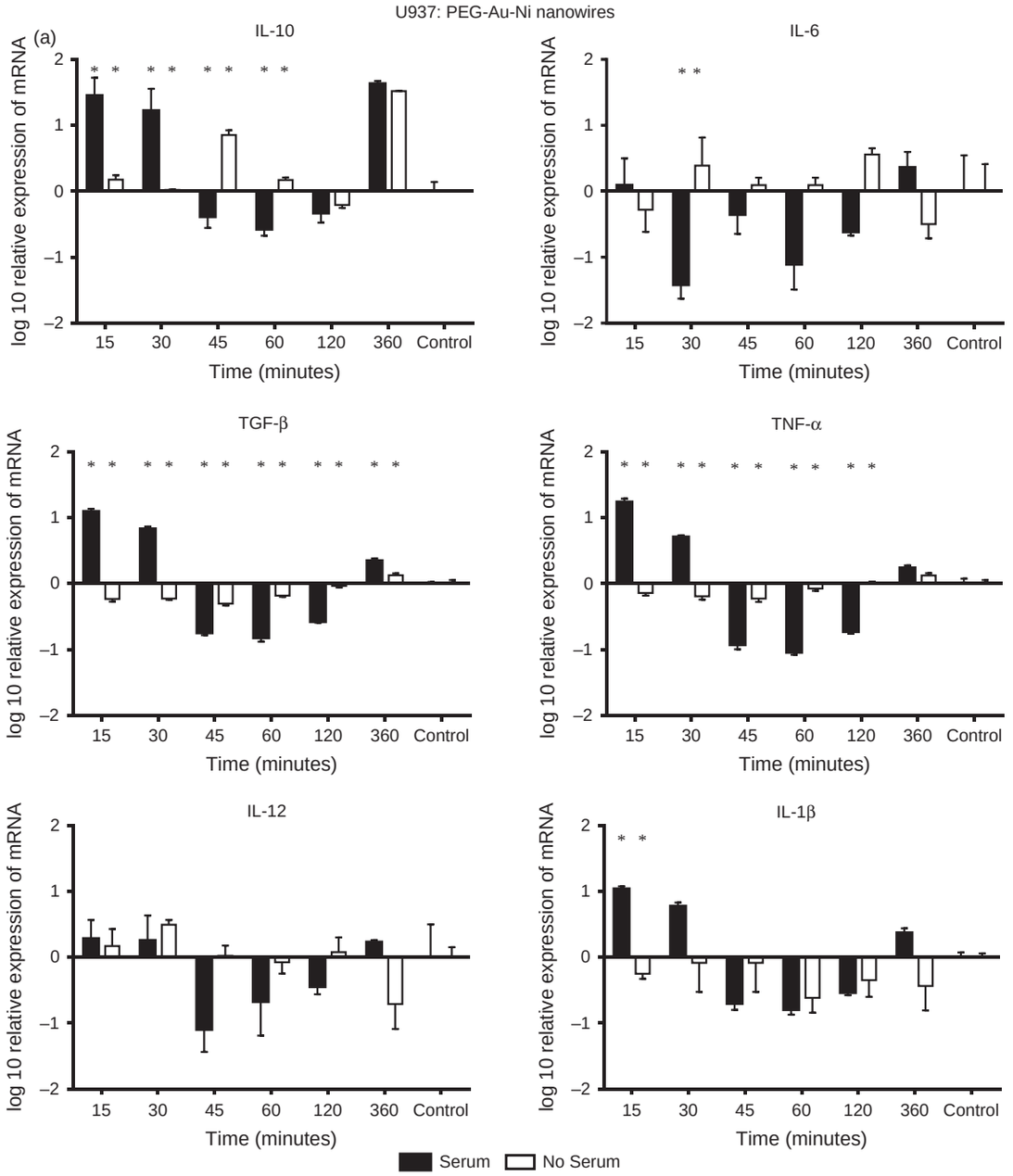

Figure 6. **Continued.**

types can influence the innate and the adaptive immune responses. IL-10 has been shown to down-regulate antigen presentation via MHC class II (HLA-DR) molecules, and pro-inflammatory cytokine/chemokine secretion through an autocrine negative-feedback loop.[58] IL-10 released by macrophages can down-regulate inducible Nitric Oxide Synthase (iNOS), Reactive Oxygen Intermediates (ROI), T cell cytokine release, and MHC expression. IL-10 is also linked with anergy induction and regulatory T cell (Treg) cell maturation in addition to dampening DC activation and subsequent cytokine release. Being an anti-inflammatory cytokine, IL-10 is likely to have an important role in limiting the immune response to nanoparticles that may otherwise cause injury and inflammation. Activation of TLR or NOD2 signalling pathways can lead to high levels of IL-10 production which can be further regulated by NF-κB.[59] Further work is required to understand the partnership between PRR and signalling pathways triggering diverse transcriptional activation that leads to

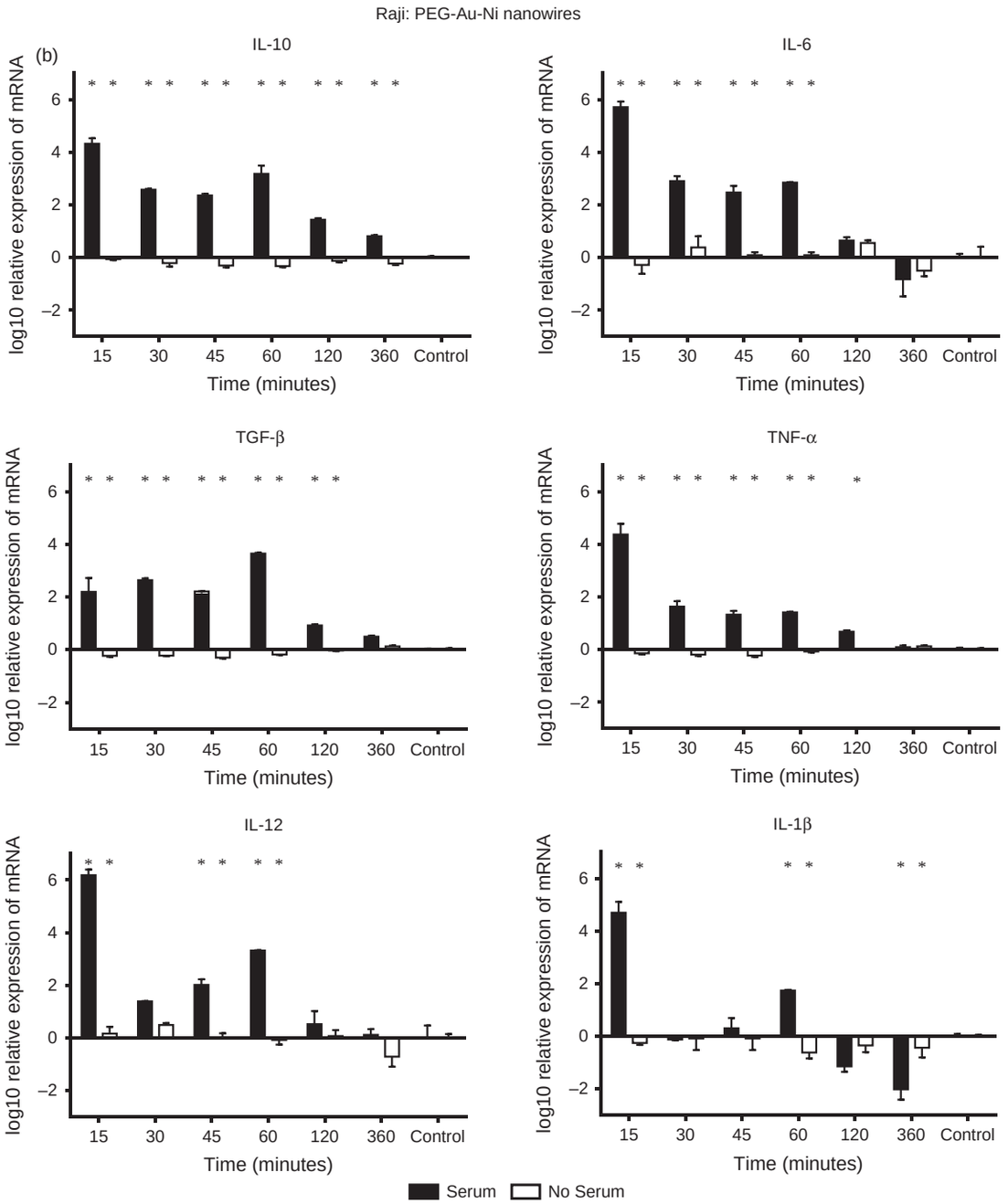

Figure 6. **Continued.**

nanoparticle-induced IL-10 production and its enhancement by complement deposition.

Another issue that is central to immune response to CNT-complement deposition is the upregulation of IL-12. Secreted by macrophages and DCs, IL-12 is an obligate requirement for Th1 cell proliferation and maturation that can cause T cell cytotoxicity and B cell activation. IL-12, in the presence of IL-18, promotes Th1 phenotypic development that is characterized by IFN-γ producing T helper type 1 (Th1) effector cells. IFN-γ drives macrophage priming and activation and adhesion molecule expression. IFN-γ eventually may retard tissue destruction, perhaps by suppressing osteoclast activation. IL-12 and IL-10 mediated effects due to complement deposition may be limiting the cytokine storm generated by the immune cells studied here.

In conclusion, this study highlights the requirement to carefully consider the nature of interactions of nanoparticles

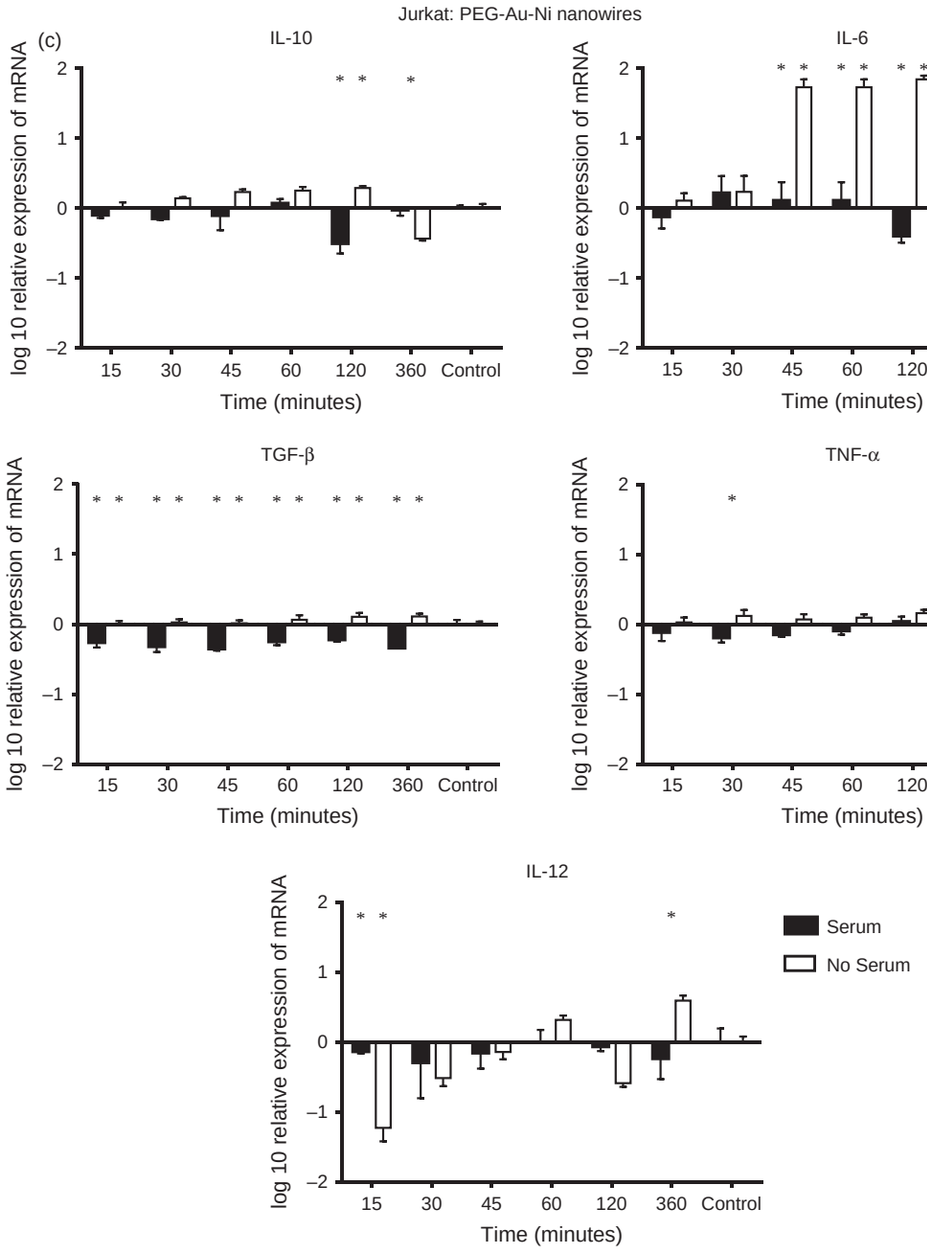

Figure 6. **qPCR analysis of the PEG-Au–Ni nanowire induced expression of cytokines by (a) U937, (b) Raji, and (c) Jurkat cell lines. For measuring anti-inflammatory and pro-inflammatory cytokines, cells were incubated with PEG-Au–Ni nanowires that were treated with serum or not treated and samples were collected at the following time-points: 15, 30, 45, 60, 120 and 360 mins. In control experiments, cells were incubated with PBS only for 30 mins. The expression of cytokine transcripts was measured using real-time qPCR and the data was normalized to 18S rRNA gene expression that was considered as an endogenous control. Assays were conducted in triplicate. Error bars represent ± standard error of the mean. A 2-way ANOVA was performed on the data to determine significant differences in expression as noted by *: $p \leq 0.05$; **: $p \leq 0.01$).**

with the complement system that in turn can impact upon the innate and adaptive immune responses. An altered charge or chemical pattern can lead to an entirely different set of immune response by antigen capturing and presenting cells such as macrophages and DCs, B and T cells, which can ultimately modify the intended outcome of nanotherapeutics. Thus, nanoparticles need to be characterized carefully for their surface molecular patterns, their ability to activate complement and their potential to generate a harmful cytokine storm by a range of immune cells.

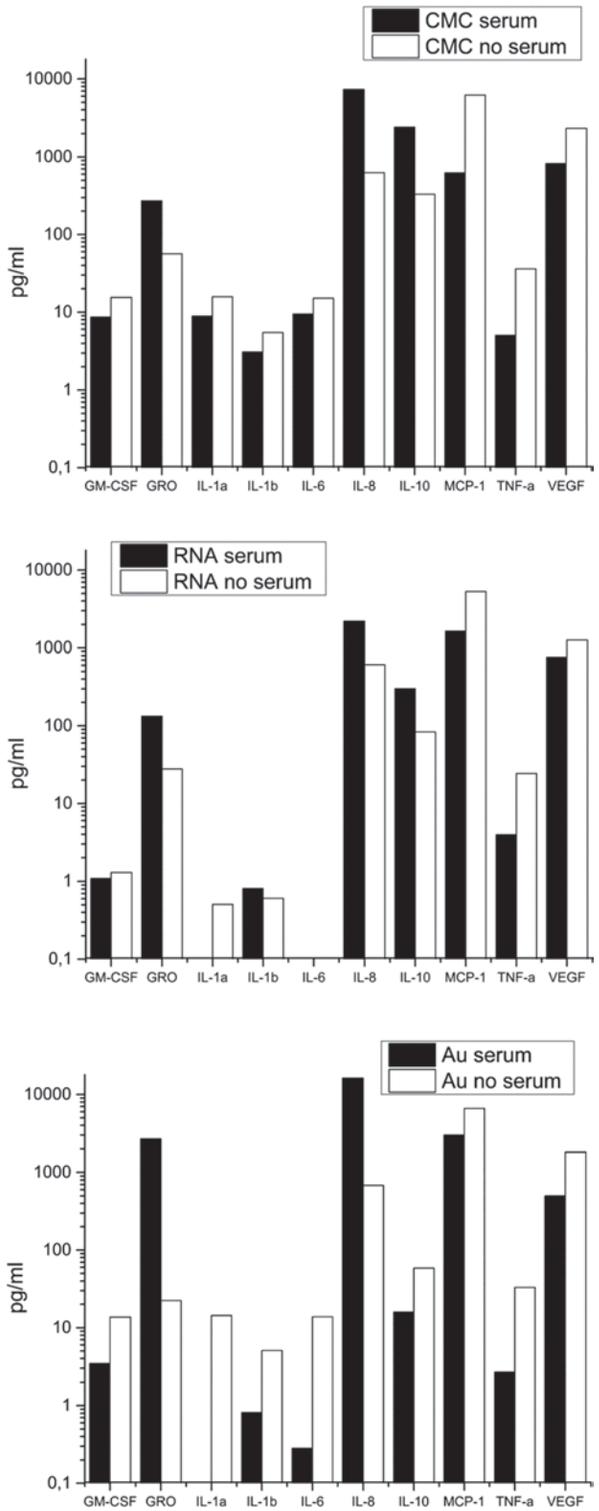

Figure 7. Multiplex cytokine array analysis of the supernatants of U937 cells treated with CMC-CNTs, RNA-CNTs or PEG-Au–Ni nanowires for 24 h. Cytokines (IL-1α, IL-1β, IL-6, IL-8, IL-10, and TNF-α) and chemokines/growth factor (MCP-1, VEGF, GM-CSF and GRO) concentrations were measured by a commercially available MagPix Milliplex kit (EMD Millipore).

Acknowledgments: Research was supported in part by the European Network CARBIO, Contract MRTN-CT-2006-035616. AT, UK, AP and GS sincerely acknowledge the Infrastructure funding by the Brunel University London.

REFERENCES

1. L. Y. Rizzo, B. Theek, G. Storm, F. Kiessling, and T. Lammers, Recent progress in nanomedicine: Therapeutic, diagnostic and theranostic applications. *Curr. Opin. Biotechnol.* 24, 1159 (**2013**).
2. M. J. Akhtar, M. Ahamed, H. A. Alhadlaq, S. A. Alrokayan, and S. Kumar, Targeted anticancer therapy: Overexpressed receptors and nanotechnology, *Clin. Chim. Acta.* 436, 78 (**2014**).
3. J. Verma, S. Lal, and C. J. Van Noorden, Nanoparticles for hyperthermic therapy: Synthesis strategies and applications in glioblastoma. *Int. J. Nanomedicine.* 9, 2863 (**2014**).
4. A. Viscido, A. Capannolo, G. Latella, R. Caprilli, and G. Frieri, Nanotechnology in the treatment of inflammatory bowel diseases. *J. Crohns. Colitis.* 8, 903 (**2014**).
5. S. E. Leucuta, Subcellular drug targeting, pharmacokinetics and bioavailability. *J. Drug Target.* 22, 95 (**2014**).
6. Q. Jiao, L. Li, Q. Mu, and Q. Zhang, Immunomodulation of nanoparticles in nanomedicine applications. *Biomed. Res. Int.* 2014, 426028 (**2014**).
7. A. Singh, M. Talekar, A. Raikar, and M. Amiji, Macrophage-targeted delivery systems for nucleic acid therapy of inflammatory diseases. *J. Control Release.* 190, 515 (**2014**).
8. H. Xu, Z. Li, and J. Si, Nanocarriers in gene therapy: A review. *J. Biomed. Nanotechnol.* 10, 3483 (**2014**).
9. Z. Liu, S. Tabakman, K. Welsher, and H. Dai, Carbon nanotubes in biology and medicine: *In vitro* and *in vivo* detection, imaging and drug delivery. *Nano Res.* 2, 85 (**2009**).
10. A. Bianco, K. Kostarelos, C. D. Partidos, and M. Prato, Biomedical applications of functionalised carbon nanotubes. *Chemical Communications.* 5, 571 (**2005**).
11. M. Foldvari and M. Bagonluri, Carbon nanotubes as functional excipients for nanomedicines: II. Drug delivery and biocompatibility issues. *Nanomedicine.* 4, 183 (**2008**).
12. R. Klingeler, S. Hampel, and B. Buchner, Carbon nanotube based biomedical agents for heating, temperature sensoring and drug delivery. *Int. J. Hyperthermia.* 24, 496 (**2008**).
13. A. Bianco, K. Kostarelos, and M. Prato, Applications of carbon nanotubes in drug delivery. *Curr. Opin. Chemical Biology.* 9, 674 (**2005**).
14. H. Ali-Boucetta, K. T. Al-Jamal, D. McCarthy, M. Prato, A. Bianco, and K. Kostarelos, Multiwalled carbon nanotube-doxorubicin supramolecular complexes for cancer therapeutics. *Chem. Commun. (Camb).* 4, 459 (**2008**).
15. E. Heister, V. Neves, C. Tîlmaciu, K. Lipert, V. S. Beltrán, H. M. Coley, S. R. P. Silva, and J. McFadden, Triple functionalisation of single-walled carbon nanotubes with doxorubicin, a monoclonal antibody, and a fluorescent marker for targeted cancer therapy. *Carbon* 47, 2152 (**2009**).
16. L. Lacerda, A. Bianco, M. Prato, and K. Kostarelos, Carbon nanotubes as nanomedicines: From toxicology to pharmacology. *Adv. Drug Deliv. Rev.* 58, 1460 (**2006**).
17. J. T. Robinson, K. Welsher, S. M. Tabakman, S. P. Sherlock, H. Wang, R. Luong, and H. Dai, High Performance *in vivo* near-IR (> 1 μm) imaging and photothermal cancer therapy with carbon nanotubes. *Nano Res.* 3, 779 (**2010**).
18. K. Welsher, S. P. Sherlock, and H. Dai, Deep-tissue anatomical imaging of mice using carbon nanotube fluorophores in the second near-infrared window. *Proc. Natl. Acad. Sci. U. S. A.* 108, 8943 (**2011**).

19. B. S. Zolnik, A. Gonzalez-Fernandez, N. Sadrieh, and M. A. Dobrovolskaia, minireview: nanoparticles and the immune system. *Endocrinology.* 151, 458 **(2010)**.

20. S. Hussain, J. A. J. Vanoirbeek, and P. H. M. Hoet, Interactions of nanomaterials with the immune system. *Wiley Interdiscip. Rev. Nanomed. Nanobiotechnol.* 4, 169 **(2012)**.

21. C. Salvador-Morales, E. V. Basiuk, V. A. Basiuk, M. L. H. Green, and R. B. Sim, Effects of covalent functionalization on the biocompatibility characteristics of multi-walled carbon nanotubes. *J. Nanosci. Nanotechnol.* 8, 2347 **(2008)**.

22. C. Salvador-Morales, E. Flahaut, E. Sim, J. Sloan, M. L. H. Green, and R. B. Sim, Complement activation and protein adsorption by carbon nanotubes. *Mol. Immunol.* 43, 193 **(2006)**.

23. M. J. Rybak-Smith, K. M. Pondman, E. Flahaut, C. Salvador-Morales, and R. B. Sim, Carbon Nanotubes for Biomedical Applications, edited by R. S. Klingeler and B. Robert, Springer, London **(2011)**.

24. M. V. Carroll and R. B. Sim, Complement in health and disease. *Adv. Drug Deliv. Rev.* 63, 965 **(2011)**.

25. R. Ghai, P. Waters, L. T. Roumenina, M. Gadjeva, M. S. Kojouharova, K. B. M. Reid, R. B. Sim, and U. Kishore, C1q and its growing family. *Immunobiology.* 212, 253 **(2007)**.

26. I. Hamad, A. C. Hunter, K. J. Rutt, Z. Liu, H. Dai, and S. M. Moghimi, Complement activation by PEGylated single-walled carbon nanotubes is independent of C1q and alternative pathway turnover. *Mol. Immunol.* 45, 3797 **(2008)**.

27. M. J. Rybak-Smith, C. Tripisciano, E. Borowiak-Palen, C. Lamprecht, and R. B. Sim, Effect of functionalization of carbon nanotubes with psychosine on complement activation and protein adsorption, *J. Biomed. Nanotechnol.* 7, 830 **(2011)**.

28. K. M. Pondman, M. Sobik, A. Nayak, A. G. Tsolaki, A. Jakel, E. Flahaut, S. Hampel, B. Ten Haken, R. B. Sim, and U. Kishore, Complement activation by carbon nanotubes and its influence on the phagocytosis and cytokine response by macrophages. *Nanomedicine.* 10, 1287 **(2014)**.

29. C. Salvador-Morales, E. Flahaut, E. Sim, J. Sloan, M. L. Green, and R. B. Sim, Complement activation and protein adsorption by carbon nanotubes. *Mol. Immunol.* 43, 193 **(2006)**.

30. C. Salvador-Morales, M. L. H. Green, and R. B. Sim, Chemistry of carbon nanotubes, edited by E. V. Basiuk and V. A. Basiuk, American Scientific Publishers, California **(2007)**.

31. K. Bhattacharya, F. T. Andon, R. El-Sayed, and B. Fadeel, Mechanisms of carbon nanotube-induced toxicity: Focus on pulmonary inflammation. *Adv. Drug Deliv Rev.* 65, 2087 **(2013)**.

32. V. A. Basiuk, C. Salvador-Morales, E. V. Basiuk, R. M. J. Jacobs, M. Ward, B. T. Chu, R. B. Sim, and M. L. H. Green, 'Green' derivatization of carbon nanotubes with Nylon 6 and L-alanine. *J. Mat. Chem.* 16, 4420 **(2006)**.

33. H. Dumortier, S. Lacotte, G. Pastorin, R. Marega, W. Wu, D. Bonifazi, J. P. Briand, M. Prato, S. Muller, and A. Bianco, Functionalized carbon nanotubes are non-cytotoxic and preserve the functionality of primary immune cells, *Nano Letters.* 6, 3003 **(2006)**.

34. M. Bottini, N. Rosato, and N. Bottini, PEG-Modified Carbon nanotubes in biomedicine: Current status and challenges ahead. *Biomacromolecules.* 12, 3381 **(2011)**.

35. A. J. Andersen, J. T. Robinson, H. J. Dai, A. C. Hunter, T. L. Andresen, and S. M. Moghimi, Single-walled carbon nanotube surface control of complement recognition and activation. *ACS Nano.* 7, 1108 **(2013)**.

36. A. J. Andersen, P. P. Wibroe, and S. M. Moghimi, Perspectives on carbon nanotube-mediated adverse immune effects. *Adv. Drug. Deliv. Rev.* 64, 1700 **(2012)**.

37. W. L. Ling, A. Biro, I. Bally, P. Tacnet, A. Deniaud, E. Doris, P. Frachet, G. Schoehn, E. Pebay-Peyroula, and G. J. Arlaud, Proteins of the innate immune system crystallize on carbon nanotubes but are not activated. *ACS Nano.* 5, 730 **(2011)**.

38. S. M. Moghimi and A. C. Hunter, Complement monitoring of carbon nanotubes. *Nat. Nanotechnol.* 5, 382 **(2010)**.

39. M. J. Rybak-Smith and R. B. Sim, Complement activation by carbon nanotubes. *Adv. Drug Deliv. Rev.* 63, 1031 **(2011)**.

40. F. A. Murphy, C. A. Poland, R. Duffin, K. T. Al-Jamal, H. Ali-Boucetta, A. Nunes, F. Byrne, A. Prina-Mello, Y. Volkov, S. Li, S. J. Mather, A. Bianco, M. Prato, W. Macnee, W. A. Wallace, K. Kostarelos, and K. Donaldson, Length-dependent retention of carbon nanotubes in the pleural space of mice initiates sustained inflammation and progressive fibrosis on the parietal pleura. *Am. J. Pathol.* 178, 2587 **(2011)**.

41. F. A. Murphy, C. A. Poland, R. Duffin, and K. Donaldson, Length-dependent pleural inflammation and parietal pleural responses after deposition of carbon nanotubes in the pulmonary airspaces of mice. *Nanotoxicology.* 7, 1157 **(2013)**.

42. F. A. Murphy, A. Schinwald, C. A. Poland, and K. Donaldson, The mechanism of pleural inflammation by long carbon nanotubes: Interaction of long fibres with macrophages stimulates them to amplify pro-inflammatory responses in mesothelial cells. *Part Fibre Toxicol.* 9, 8 **(2012)**.

43. J. Palomaki, E. Valimaki, J. Sund, M. Vippola, P. A. Clausen, K. A. Jensen, K. Savolainen, S. Matikainen, and H. Alenius, Long, needle-like carbon nanotubes and asbestos activate the NLRP3 inflammasome through a similar mechanism. *ACS Nano.* 5, 6861 **(2011)**.

44. D. Liu, L. Wang, Z. Wang, and A. Cuschieri, Different cellular response mechanisms contribute to the length-dependent cytotoxicity of multi-walled carbon nanotubes. *Nanoscale Res. Lett.* 7, 361 **(2012)**.

45. D. M. Brown, I. A. Kinloch, U. Bangert, A. H. Windle, D. M. Walter, G. S. Walker, C. A. Scotchford, K. Donaldson, and V. Stone, An *in vitro* study of the potential of carbon nanotubes and nanofibres to induce inflammatory mediators and frustrated phagocytosis. *Carbon* 45, 1743 **(2007)**.

46. E. Meunier, A. Coste, D. Olagnier, H. Authier, L. Lefevre, C. Dardenne, J. Bernad, M. Beraud, E. Flahaut, and B. Pipy, Double-walled carbon nanotubes trigger IL-1 beta release in human monocytes through Nlrp3 inflammasome activation. *Nanomedicine: Nanotechnol. Biol. Med.* 8, 987 **(2012)**.

47. M. Yang, K. Flavin, I. Kopf, G. Radics, C. H. Hearnden, G. J. McManus, B. Moran, A. Villalta-Cerdas, L. A. Echegoyen, S. Giordani, and E. C. Lavelle, Functionalization of carbon nanoparticles modulates inflammatory cell recruitment and NLRP3 inflammasome activation. *Small* 9, 4194 **(2013)**.

48. K. Kostarelos, L. Lacerda, G. Pastorin, W. Wu, S. Wieckowski, J. Luangsivilay, S. Godefroy, D. Pantarotto, J. P. Briand, S. Muller, M. Prato, and A. Bianco, Cellular uptake of functionalized carbon nanotubes is independent of functional group and cell type. *Nat. Nanotechnol.* 2, 108 **(2007)**.

49. G. Laverny, A. Casset, A. Purohit, E. Schaeffer, C. Spiegelhalter, F. de Blay, and F. Pons, Immunomodulatory properties of multi-walled carbon nanotubes in peripheral blood mononuclear cells from healthy subjects and allergic patients. *Toxicol. Lett.* 217, 91 **(2013)**.

50. A. A. Shvedova, E. Kisin, A. R. Murray, V. J. Johnson, O. Gorelik, S. Arepalli, A. F. Hubbs, R. R. Mercer, P. Keohavong, N. Sussman, J. Jin, J. Yin, S. Stone, B. T. Chen, G. Deye, A. Maynard, V. Castranova, P. A. Baron, and V. E. Kagan, Inhalation versus aspiration of single-walled carbon nanotubes in C57BL/6 mice: Inflammation, fibrosis, oxidative stress, and mutagenesis. *Am. J. Physiol. Lung Cell. Mol. Physiol.* 295, L552 **(2008)**.

51. L. Dykman and N. Khlebtsov, Gold nanoparticles in biomedical applications: Recent advances and perspectives. *Chem. Soc. Rev.* 41, 2256 **(2012)**.

52. D. A. Giljohann, D. S. Seferos, W. L. Daniel, M. D. Massich, P. C. Patel, and C. A. Mirkin, Gold nanoparticles for biology and medicine. *Angew. Chem. Int. Ed. Engl.* 49, 3280 **(2010)**.

53. M. A. Dobrovolskaia, A. K. Patri, J. Zheng, J. D. Clogston, N. Ayub, P. Aggarwal, B. W. Neun, J. B. Hall, and S. E. McNeil, Interaction of colloidal gold nanoparticles with human blood: Effects on particle

size and analysis of plasma protein binding profiles. *Nanomedicine.* 5, 106 **(2009)**.

54. K. Lipert, F. Kretzschmar, M. Ritschel, A. Leonhardt, R. Klingeler, and B. Buchner, Nonmagnetic carbon nanotubes. *J. Appl. Phys.* 105, 63906 **(2009)**.

55. K. M. Pondman, A. W. Maijenburg, F. B. Celikkol, A. A. Pathan, U. Kishore, B. T. Haken, and J. E. T. Elshof, Au coated Ni nanowires with tuneable dimensions for biomedical applications. *J. Mater. Chem. B.* 1, 6129 **(2013)**.

56. H. Haniu, N. Saito, Y. Matsuda, T. Tsukahara, K. Maruyama, Y. Usui, K. Aoki, S. Takanashi, S. Kobayashi, H. Nomura, M. Okamoto, M. Shimizu, and H. Kato, Culture medium type affects endocytosis of multi-walled carbon nanotubes in BEAS-2B cells and subsequent biological response. *Toxicol In Vitro* 27, 1679 **(2013)**.

57. C. Wagner, G. M. Hansch, S. Stegmaier, B. Denefleh, F. Hug, and M. Schoels, The complement receptor 3, CR3 (CD11b/CD18), on T lymphocytes: Activation-dependent up-regulation and regulatory function. *Eur. J. Immunol.* 31, 1173 **(2001)**.

58. S. Pestka, C. D. Krause, D. Sarkar, M. R. Walter, Y. Shi, and P. B. Fisher, Interleukin-10 and related cytokines and receptors. *Annu. Rev. Immunol.* 22, 929 **(2004)**.

59. M. Saraiva and A. O'Garra, The regulation of IL-10 production by immune cells. *Nat. Rev. Immunol.* 10, 170 **(2010)**.